Supporting Information for

Magnetite Magnetosome Biomineralization in *Magnetospirillum magneticum* strain AMB-1: a Time Course Study

Lucas Le Nagard[1,+], Xiaohui Zhu[2,#], Hao Yuan[2], Karim Benzerara,[3] Dennis A. Bazylinski,[4] Cécile Fradin[1], Adrien Besson,[5] Sufal Swaraj,[5] Stefan Stanescu,[5] Rachid Belkhou[5] and Adam P. Hitchcock[1,2,*]

AMB1-time-course-STXM-SI-REVISED.doc last changed: 13-Sep-2019

Table S-1 Summary of results from previous time course studies in magnetite biomineralization by magnetotactic bacteria in the genus *Magnetospirillum*.

Ref	species	Added Fe	Methods	~time to chains	Intermediate(s)	size	Other
2004KV&	AMB-1	Fe(III)	TEM (u-tome); genetics	Small ~2h Large, full chains ~20 h	"none"	Small & large	Pre-formed lipid vesicles in Fe-starved cells, mamA required
2007FB&	MSR-1	Fe(II), Fe(III)	Mossbauer	~6 h	Ferritin, Fe(II); direct to msomes		
2007JS	MSR-1		Mossbauer	~6 h			
2007SW&	MSR-1	Fe(III)	TEM; **mag-OD**; XAS & XMCD on m'some extracts with applied H	~15 m	α-hematite at surface only in 1st 15 m	All large	No-Fe grown with 5% O_2
2008FM&	MSR-1	Fe(III)	TEM	Small ~ 100 min Long ~ 6h		Small then large (50 min lag time)	Late time-course samples and "normal" cultures have different msome size distribution ➔ crystal growth after induction is too fast for optimal biological control.
2009LP&	AMB-1	Fe(III)	TEM (whole extracts); size dist.; **magnetism(T)**	~20 h lag phase; 96 h full	(no comment)	Small, large	TEM images similar to this work; 10 h MINIMUM sample – few msomes, all small

2012MF&	AMB-1	Fe(III)malate	Genetics (ΔMmsF), ET, TEM	30, 90, 150 and 270 m	(no comment)	small	MmsF regulates biomineralization – 20 nm magnetite induced when added to preformed membrane-organelle
2013FM&	MSR-1	Fe(III)	Fe K-edge XANES; TEM	Small ~3h Long >6h	(Phosphorus-rich) Ferrihydrite	Medium, large	ferrihydrite precursors observed with HRTEM. Attributd to low density. Quantitative measurement of ferrihydrite&magnetite content over time.
2013BM&	AMB-1	Fe(III)	Fe K-edge XAS (shows 2 types of Fe), EXAFS; Magnetism from magnetically induced differential light scattering; TEM, XRD	10 m first sampling ~2 h to start msomes; complete at 46 h	phosphate-rich ferric hydroxide phase (ferritin-like) with transient Fe(III)		Mimics synthetic magnetite formation Magnetic response after 80-100 m
2016FP&	AMB-1	Fe(III)	HAADF-TEM, TEM-EELS (Fe L3, O K), ED, size dist.	30 m - small, no chain 1 d mix small, large	Amorphous, Fe(III) - perhaps Fe(OH)3 Fe(III)-rich (2-line ferrihydrite)	Small, large	
2019FO&	AMB-1		In situ TEM graphene liquid cell ; EELS, ED	17 m, 31 m	Fe(III) rich; hematite surface layer	small	In situ growth ➔ 'living cells'
2019WZ&	MSR-1	Fe(III)	TEM, ED	0,5,10,15, 25 m	ε-Fe_2O_3	v. small	ε-Fe_2O_3 is a low stability phase
This work	AMB-1	Fe(III)	TEM; **TEY**-XAS & XMCD microscopy	~2 – 4 h	Fe(III) α-hematite	Small then large	No-Fe grown with 20% O_2

References

2004KV& Komeili A, Vali H, Beveridge TJ, Newman DK (2004) Magnetosome vesicles are present before magnetite formation, and MamA is required for their activation Proc Natl Acad Sci USA 101, 3839–3844.

2007FB& Faivre, D., Böttger, L.H., Matzanke, B.F., Schüler, D. (2007) Intracellular Magnetite Biomineralization in Bacteria Proceeds by a Distinct Pathway Involving Membrane-Bound Ferritin and an Iron(II) Species, Angew. Chem., Int. Ed. Engl 46, 8495-8499.

2007JS C. Jogler and D. Schüler, in *Genetic Analysis of Magnetosome Biomineralization BT – Magnetoreception and Magnetosomes in Bacteria,* ed. D. Schüler, Springer Berlin Heidelberg, Berlin, Heidelberg, 2007, pp. 133–161.

2007SW& Staniland, S., Ward, B., Harrison, A., van der Laan, G., Telling, N. (2007) Rapid magnetosome formation shown by real-time x-ray magnetic circular dichroism, Proc. Nat. Acad. Sci. 104, 19524-19528.

2008FM& Faivre, D., Menguy, N., Pósfai, M., & Schüler, D. (2008). Environmental parameters affect the physical properties of fast-growing magnetosomes. American Mineralogist, 93(2-3), 463-469.

2009LP& Li, J., Pan, Y.X. , Chen, G., Liu, Q., Tian, L.X., Lin , W. (2009) Magnetite magnetosome and fragmental chain formation of Magnetospirillum magneticum AMB-1: Transmission electron microscopy and magnetic observations, Geophys. J. Int. 177, 33-42.

2012MF& Murat D., Falahati V., Bertinetti L., Csencsits R., Körnig A., Downing K., Faivre D., Komeili A. (2012) The magnetosome membrane protein, MmsF, is a major regulator of magnetite biomineralization in Magnetospirillum magneticum AMB-1, Molecular Microbiology 85, 684-699.

2013BM& Baumgartner, J., Morin, G., Menguy, N. Gonzalez, T.P., Widdrat, M., Cosmidis, J., Faivre, D., (2013) Magnetotactic bacteria form magnetite from a phosphate-rich ferric hydroxide via nanometric ferric (oxyhydr)oxide intermediates, P.N.A.S. 110, 14883–14888

2013FM& Fedez-Gubieda, M. L., Muela, A., Alonso, J., García-Prieto, A., Olivi, L., Fernández-Pacheco, R., & Barandiarán, J. M. (2013). Magnetite biomineralization in Magnetospirillum gryphiswaldense: time-resolved magnetic and structural studies. ACS nano, 7(4), 3297-3305.

2016FP& Firlar, E., Perez-Gonzalez, T.,Olszewska, A., Faivre, D., Prozorov, T., (2016) Following iron speciation in the early stages of magnetite magnetosome biomineralization, J. Mater. Res. 31, 547-555

2019FO& Firlar, E.,Ouy, M., Bogdanowicz, A., Covnot, L., Song, B., Nadkarni, Y., Shahbazian-Yassar, R., Shokuhfar T. (2019) Investigation of the magnetosome biomineralization in magnetotactic bacteria using graphene liquid cell – transmission electron microscopy, Nanoscale 11, 698-705.

2019WZ& Wen, T., Zhang,Y., GengY., Liu, J., Basit, A., Tian, J., Li, Y., Li, J., Ju, J., Jiang, W. (2019) Epsilon-Fe_2O_3 is a novel intermediate for magnetite biosynthesis in magnetotactic bacteria, . Biomaterials Research 23, 13 (1-7).

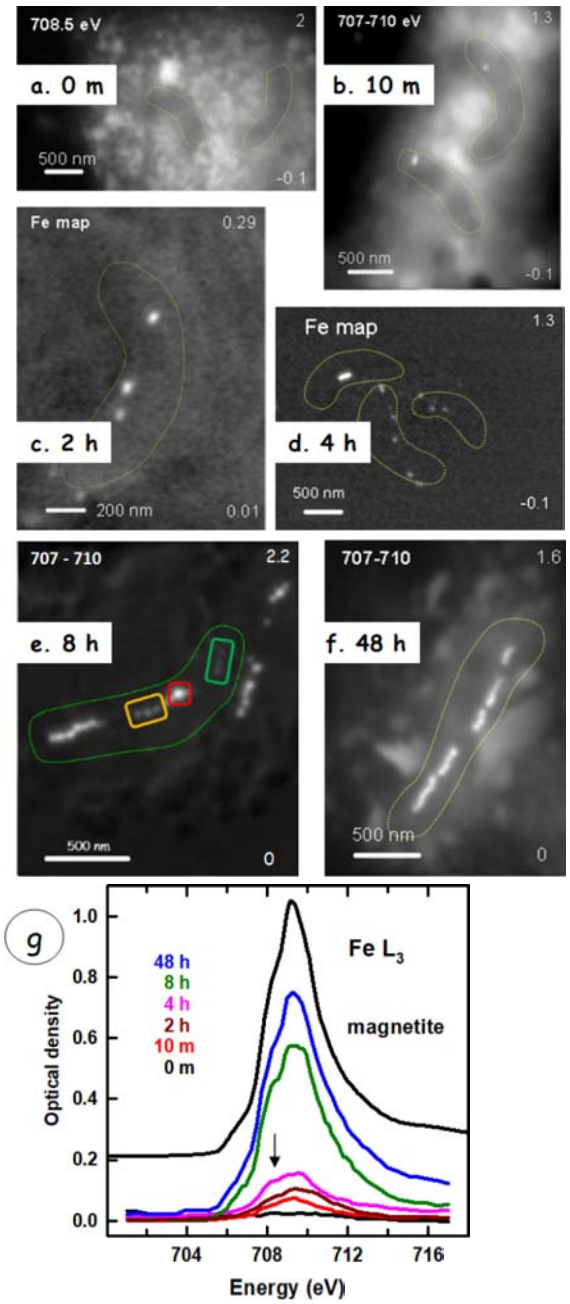

Figure S-1 Results from time course batch A. (a-f) STXM images of cells from the indicated time points. For 10 minute (m), 8 hour (h), 48 h the image is average of 12 OD images from 707-710 eV. For 0 m it is an $OD_{708.5}$ image. For the 2 h and 4 h Fe maps, differential optical density images ($OD_{710} - OD_{707}$) are displayed. (g) Average Fe L_3 spectra of all particles in the 6 time point samples in (a-f), compared to the average of CL and CR spectra of synthetic magnetite (Goering et al 2007).

Table S-2 Distribution of magnetosomes per cell as a function of time in the time course determined from TEM imaging

	10-20 nm	20-30 nm	30-40 nm	>40 nm	Total
10 min (n=18)	3 ± 1.9	2.1 ± 1.7	1.5 ± 1.8	0.7 ± 0.8	7.3 ± 3.2
30 min (n=19)	3.5 ± 2.1	1.6 ± 1.5	1.1 ± 1.2	1.1 ± 1.6	7.2 ± 3.8
1 h (n=20)	5.9 ± 4.4	1.7 ± 1.2	1.3 ± 1.5	1.1 ± 1.1	10 ± 6.3
2 h (n=20)	9.4 ± 4.7	1.9 ± 2.3	0.9 ± 1.1	0.3 ± 0.5	12.4 ± 5.9
4 h (n=19)	7.3 ± 3.1	4.6 ± 3.3	2.9 ± 1.6	2.8 ± 2.8	17.6 ± 5.6
6 h (n=20)	7.1 ± 3	4 ± 1.5	3.1 ± 1.8	6.4 ± 2.8	20.6 ± 4.6
8 h (n=20)	6.8 ± 3.4	5.3 ± 2.8	4.1 ± 1.8	8.9 ± 3.2	25 ± 6.3
24 h (n=21)	7.1 ± 3.2	4.7 ± 2.1	4.5 ± 2.3	10.2 ± 3.6	26.5 ± 7.9
48 h (n=20)	6.7 ± 2.3	3.8 ± 2	4.5 ± 2.1	12.4 ± 3.3	27.3 ± 6.2

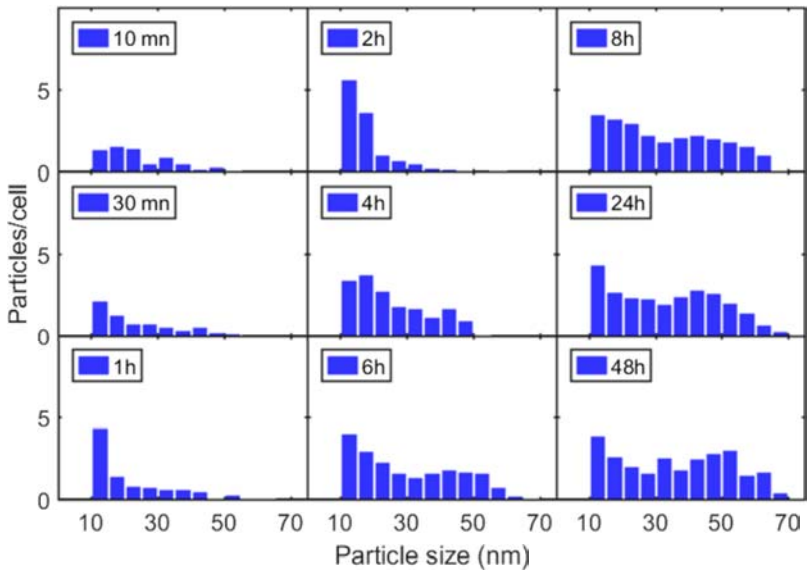

Figure S-2 Plot of size distribution of particles per cell at each of the 9 time course points in batch B, as observed by TEM.

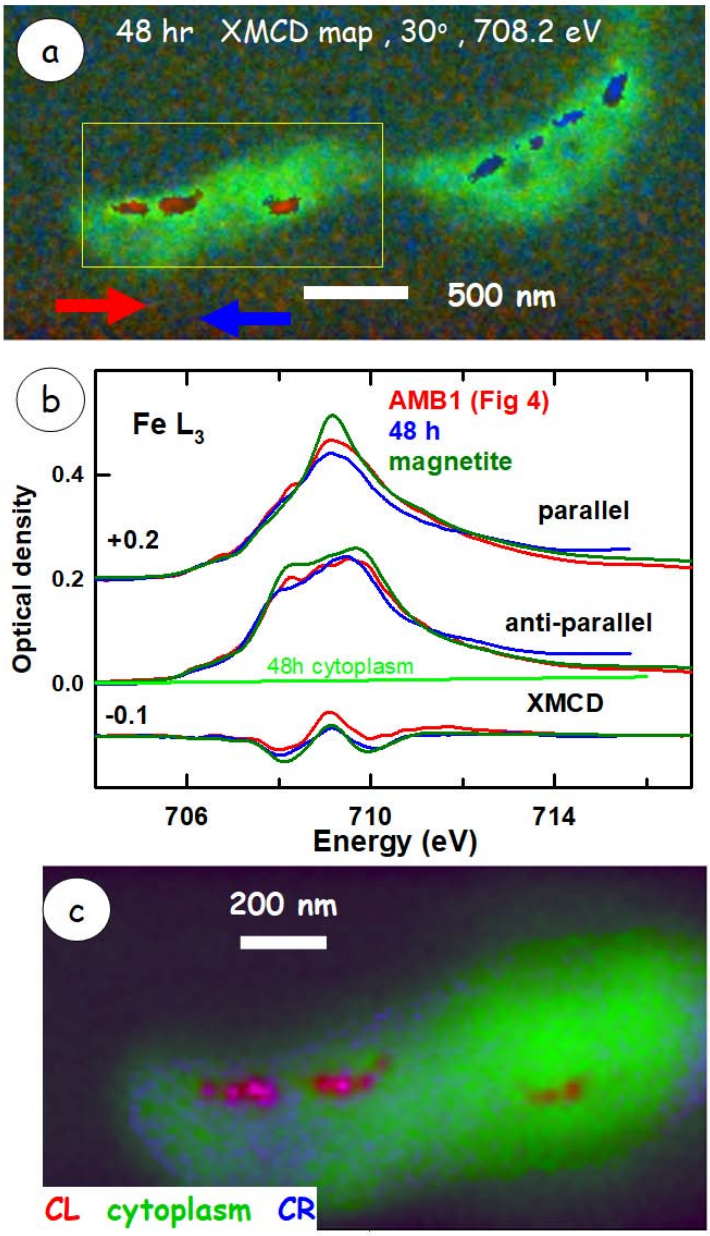

Figure S-3. 48 h sample from batch B. (a) XMCD map (CR – CL, for 708.2 eV) of 2 cells. Note that the magnetic moment of the left and right cells are opposite to each other. (b) Plot of spectra of magnetosomes with parallel, anti-parallel and XMCD (with indicated offsets) for (i) AMB-1 cells from a high Fe content culture of AMB-1 grown over an extended time period (Fig. 4), (ii) 48 h, (iii) corresponding data for magnetite (Goering *et al.* 2007). The spectrum of the cytoplasm for the 48 h sample is also plotted. (c) Color coded composite of component maps of XMCD (CR - red, CL - blue) and cytoplasm signal (green).

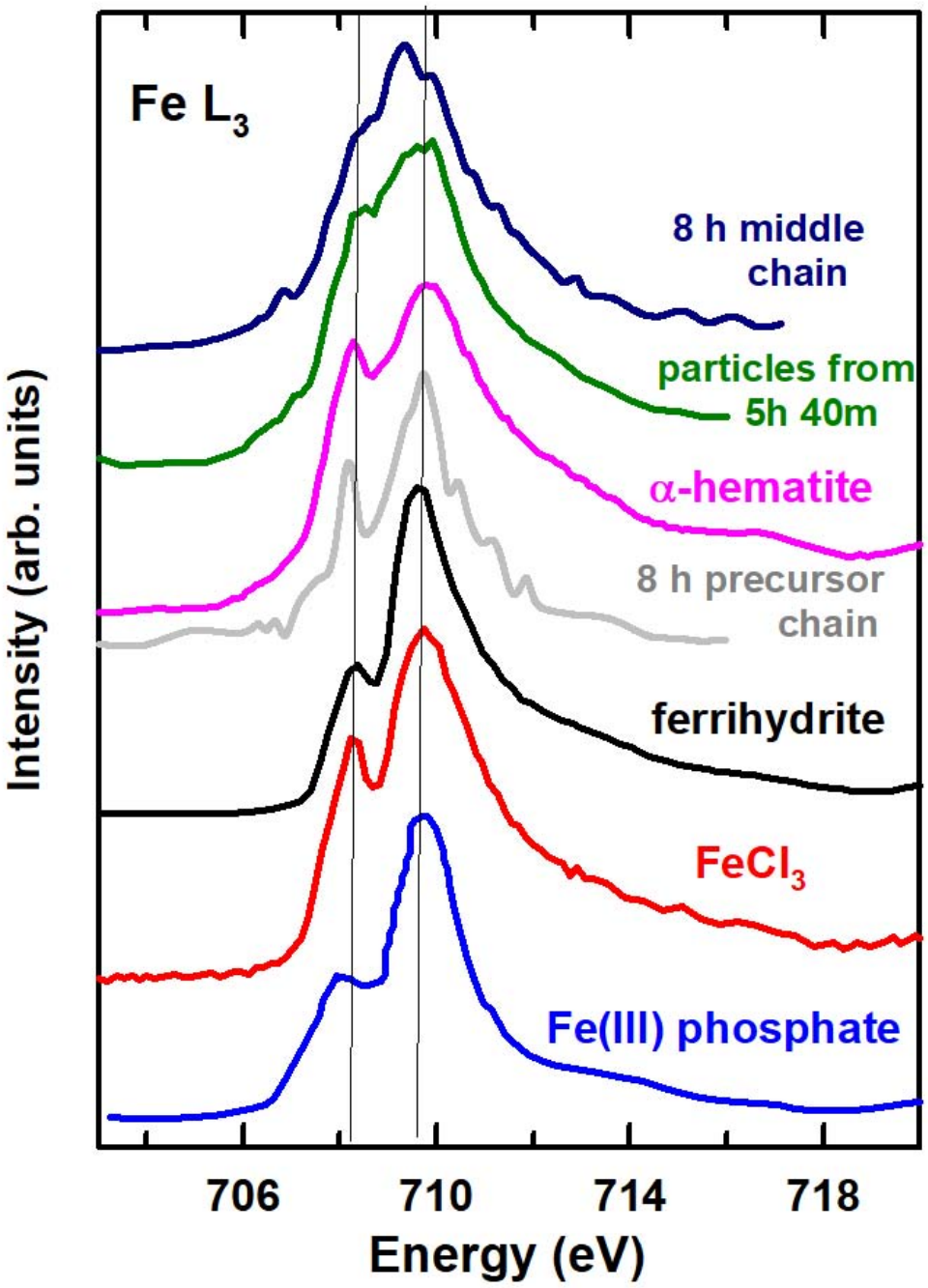

Figure S-4. Fe L_3 spectra of partly oxidized particles from 5 h 40 m sample (Fig. 6), and those of the precursor and 'middle' chains from the 8 h sample (Fig. 5) compared to the spectra of α-hematite (Zhu et al, 2015), ferrihydrite (Joshi et al 2018), $FeCl_3$ (Nagasaka, et al 2013) and Fe(III) phosphate (Miot et al, 2009).

Supplemental Fig. S-5 presents results from a cell of the 4 h sample of batch B. **Figure S-6a** represents the average of 22 OD-converted images of the same region measured between 707 and 711 eV using CL polarization. **Figure S-5b** is the particle component map derived from a fit of the Fe L_3 stack (recorded using CR polarization) to the spectra of the cytoplasm (which did not exhibit an Fe 2 p signal) and to that of the small particles visible in Fig. S-3a. This cell contains a large (~40 nm diameter) particle and thus, likely a mature magnetosome, and 4-6 smaller particles. These small crystals appear to be 25-30 nm in diameter, but could be smaller since imaging is limited by the focusing properties of the 30 nm ZP used. **Figure S-5c** presents the XAS and XMCD Fe L_3 spectra of the large magnetosome measured with the sample normal to the X-ray beam (tilt = 0^o). The large magnetosome exhibits noisy yet detectable XMCD, despite the fact that in studies of cells grown in high Fe medium, one only sees the magnetic signal when the sample, and thus the plane of the cell, is tilted out of the plane. In contrast the small particles do not show measurable XMCD, either because they are not magnetite (α-hematite is antiferromagnetic, with no XMCD), or because they do not yet possess a permanent magnetic moment, or because the geometry used (tilt = 0°, where there is no XMCD from in-plane magnetic moments) hindered their detection. To observe an XMCD signal, a non-zero projection of the magnetization vector onto the beam direction is required. An isolated magnetosome such as the large particle in this cell can have its magnetic moment oriented in any direction. Since this measurement was performed with the sample normal to the X-ray beam, the presence of a detectable XMCD signal shows that the large magnetosome possesses an out-of-plane magnetization. In distinct contrast, the average spectrum of the 3 small particles shows no detectible XMCD. In addition the XAS of the 3 small particles has a distinct shoulder at 708 eV, characteristic of significant Fe(III) character (see also **Fig. S-4**).

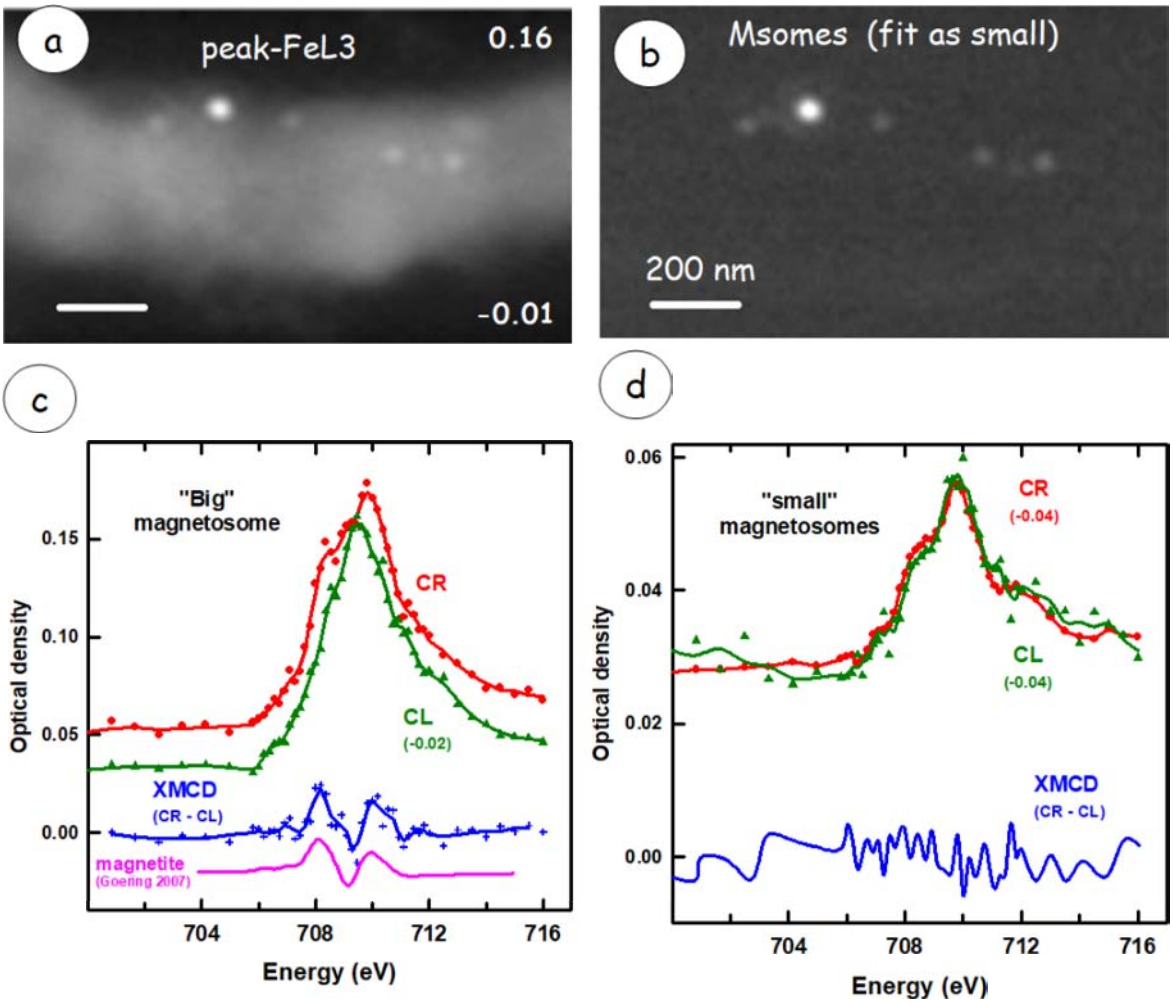

Figure S-5 4 h sample of batch B. (a) Average OD image from 707.5 – 711 eV (CL). (b) Component map of particles (CR) derived from fit to the Fe L_3 spectrum of the 4 small particles. (c) XAS and XMCD of the single large magnetosome. (d) average XAS and XMCD of the four small particles. For these measurements the sample plate was orthogonal to the X-ray beam propagation direction (tilt angle = 0^{o}).

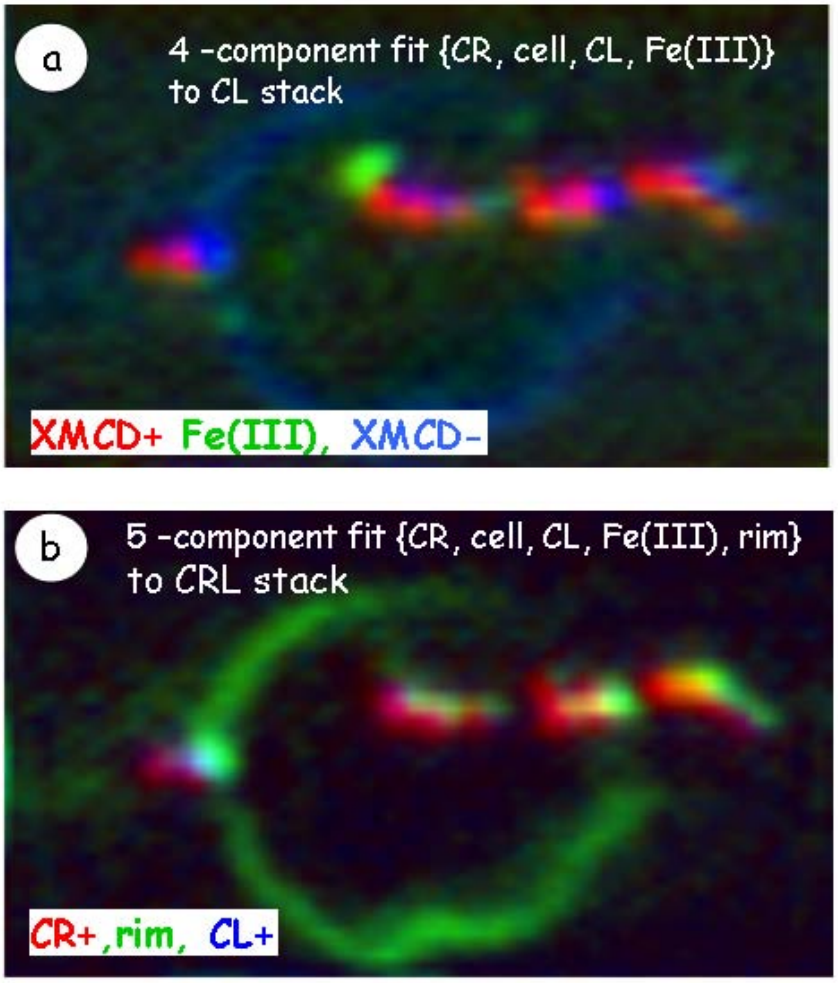

Figure S-6 Comparison of two approaches to analyze the Fe L_3 stack of the 24 h sample of batch B. Fig. 8 of the main paper presents the full Fe 2p spectra of the particles and the 'rim' where the CR and CL spectra are taken from the same area, but with opposite polarization. **(a)** is a color coded composite from a 4-component fit on the CL stack using internal reference spectra for CR, CL, cytoplasm and Fe(III). A specific signal for 'rim' component was not included and the rim shows up in the CL signal. (b) is a color coded composite from a 5-component fit to the CR stack using CR and CL spectra presented in Fig 8, cytoplasm, Fe(III) and the spectrum of the rim region. In this fit the rim component is clearly observed. Note the rim region does not exhibit XMCD – see **Fig. S-7**). The rim component also maps to parts of the magnetosome chain. This analysis procedure supports out speculation that the rim region may be precursor iron not yet incorporated into particles.

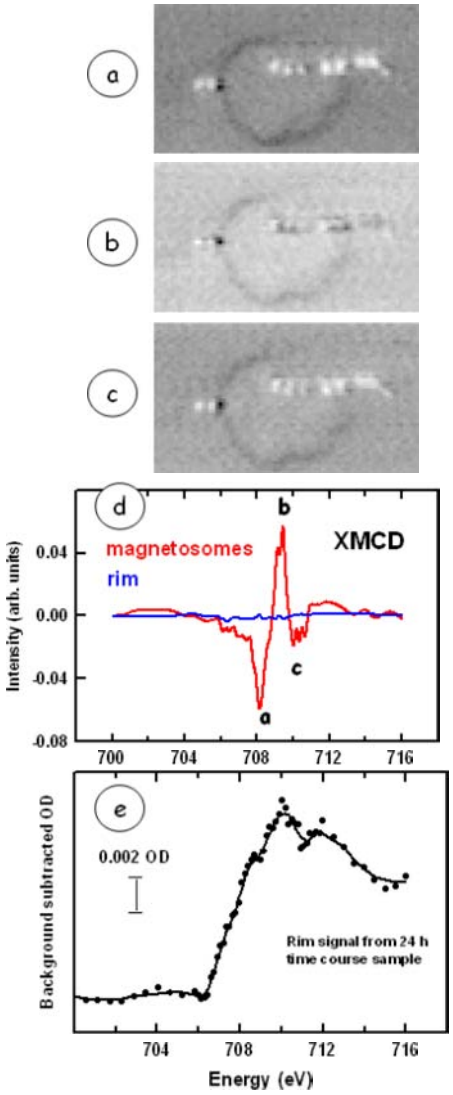

Figure S-7 Fe L_3 results for 24 h sample of batch B. (a-c) Images from the XMCD map (CR – CL) measured with the sample at a 30^o tilt., at energies a, b, c indicated in **S-7d**. (d) extracted XMCD spectra of the particles and the 'rim'. (e) Linear background subtracted Fe L_3 spectrum of the 'rim'. See Fig. 8 of the main paper for the full Fe 2p spectra of the particles and the 'rim'.